LWS observations of the bright rimmed globule IC1396N[*]

P. Saraceno[1,2], C. Ceccarelli[1,2], P. Clegg[3], C. Correia[3], A. Di Giorgio[4], T. Giannini[1], M. Griffin[3], D. Lorenzetti[5], S. Molinari[1,4], Nguyen-Q-Rieu[6], B. Nisini[1], A. Radicchi[1], L. Spinoglio[1], E. Tommasi[1], G.J. White[3], P.A.R. Ade[3], P. André[7], C. Armand[4], M.J. Barlow[8], M. Burgdorf[4], E. Caux[9], P. Cerulli[1], J. Fischer[10], I. Furniss[8], B. Glencross[8], C. Gry[4], K.J. King[15], T. Lim[4], R. Liseau[1,11], N. Minchin[3], D. Naylor[12], D. Texier[4], R. Orfei[1], F. Palla[13], S. Sidher[4], H.A. Smith[14], B. Swinyard[15], N. Trams[4], and S. Unger[15]

[1] CNR-Istituto di Fisica dello Spazio Interplanetario, CP 27, I-00044 Frascati, Italy
[2] Laboratoire d'Astrophysique de l'Observatoire de Grenoble, rue de la Piscine, BP 53, F-38041 Grenoble, France
[3] Physics Department, Queen Mary & Westfield College, University of London, Mile End Road, London E1 4NS, UK
[4] The LWS Instrument-Dedicated Team, ISO Science Operations Centre, Villafranca, Spain
[5] Osservatorio Astronomico di Roma, I-00040 Monte Porzio, Italy
[6] Observatoire de Paris, 61 avenue de l'Observatoire, F-75014 Paris, France
[7] C.E.A., Service d'Astrophysique C.E. Saclay, F-91191 Gif-sur-Ivette Cedex, France
[8] Dept. Physics and Astronomy, University College London, Gower Street, London, UK
[9] CESR/CNRS-UPS, BP 4346, F-31029 Toulouse Cedex, France
[10] Naval Research Laboratory, Remote Sensing Division, 4555 Overlook Ave., SW, Washington D.C., USA
[11] Stockholm Observatory, Saltsjöbaden, Sweden
[12] Dept. of Physics, University of Lethbridge, Lethbridge, Alberta t1k 3m4, Canada
[13] Osservatorio Astrofisico di Arcetri, Largo E.Fermi 5, I-50125 Firenze, Italy
[14] Laboratory for Astrophysics, National Air and Space Museum, Smithsonian Institution, Washington D.C., USA
[15] Space Science Department, Rutherford Appleton Lab, Chilton, Oxon OX11 OQX, UK

Abstract. We present the first far-infrared spectrum of the IRAS source associated with IC1396N, located in the HII region IC1396 together with submillimeter and millimeter photometry. A rich spectrum of CO, OH, and H_2O lines are detected in the ISO-LWS spectrum, indicative of a warm, dense region, probably shock excited, around the source. Among the fine structure lines, [OIII] and [NIII] are also detected and can be explained by the presence of the O6 star HD206267 approximately 16 pc away.

The far infrared and submillimeter spectral energy distribution is fitted with a model assuming spherical grey-bodies with a radial power law of density and temperature. An accurate measure of the bolometric luminosity and an estimate of the total envelope mass are obtained.

Key words: stars: formation – ISM: jets and outflows – ISM: individual objects: IC1396N – infrared: ISM:lines

1. Introduction

IC1396N (associated with IRAS21391+5802) is a bright rimmed globule, located at a distance of $\sim$ 16pc from the O6 star HD 206267 which excites the IC1396 HII region. This HD star is a member of the open cluster Trumpler 37 forming the nucleus of the Cep OB2 association (Simonson, 1968).

The IC1396 region, whose estimated distance is 750 pc (Matthews 1979), has been extensively studied in the past. Osterbrock (1957) showed the existence of many globules, several of which show bright H_α rims. Kun et al. (1987) found that the IRAS sources identified in the region are distributed in a ring around the O6 star indicating a star formation process induced by this source. Recently, Patel et al. (1995) surveyed IC1396 in ^{12}CO and ^{13}CO, and showed that the 12 pc ring is expanding at a velocity of 5 km s^{-1}. Ten of the globules are associated with IRAS sources, IC1396N being the brightest. Sugitani et al. (1989) discovered an extended ($\sim$ 3 arcmin) CO bipolar outflow associated with IC1396N. They also suggest that the 0.1 pc separation between IC1396N and the bright rim (tracing the ionization front) in the direction of the O6 star, indicates that the star formation has resulted from a radiation driven implosion, which occurred $\sim 10^4$ years ago. In an extensive study of bright-rimmed clouds, Sugitani et al. (1991) found that this process is expected to contribute up to 5% of the total stellar mass
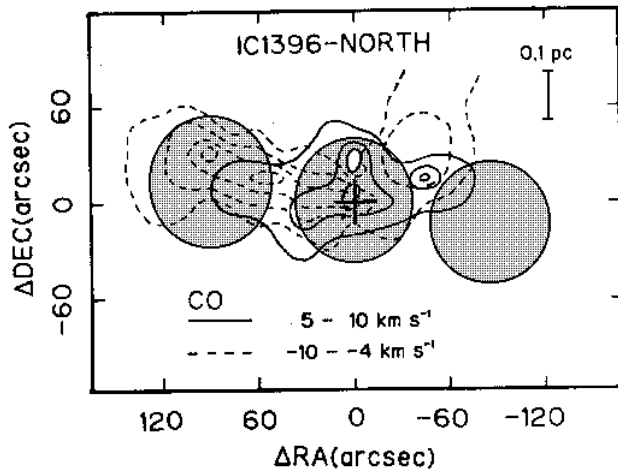
Fig. 1. CO J=1-0 map (Sugitani et al.1989), showing the red and blue lobes of the outflow. The circles represent the ISO-LWS beam at the observed positions. The *on*-source spectrum is centered on IRAS21391+5802 (α_{1950} 21^h : 39^m : 10.3^s, δ_{1950} $+58^o$: $2'$: $29''$); the two *off*-source spectra were taken at a position angle of 81°, one at 90" E, on the red and part of the blue lobes, and the second at 90" W of the main flow.

of the Galaxy, producing stars approximately 100 times brighter than those associated with dense molecular cores. Among this class of objects, IC1396N is one of the closest to the Sun, allowing with ISO-LWS the study of a case of a non quiescent star forming process.

2. Observations and results

2.1. ISO-LWS observations

The spectra of IC1396N were collected with the ISO satellite (Kessler et al.1996) on 26 February 1996 (orbit 96), with the LWS spectrometer described by Clegg et al.(1996) and Swinyard et al.(1996). The instrument was operated in the "fast scanning" grating mode (R $\sim$200) in the range 43 - 196.7 μm. The positions observed are shown in Fig.1. Each spectral element was oversampled by a factor of four, with a total integration time per sample of 7.6 sec on source (corresponding to 19 full grating scans) and 3.6 sec at the two off-source positions (corresponding to 9 full grating scans). The data were calibrated using observations of Uranus. The relative calibration accuracy on the continuum between the different detectors has been estimated to be better than 30%, based on the comparison of overlapping portions of spectra in adjacent detectors.

The spectra were cleaned of glitches due to cosmic rays and then coadded. However, the spectra of this source exhibit strong fringes which have not yet been satisfactorily removed (Swinyard et al. 1996). Because of this, we do not yet want to base any conclusions on line strengths or ratios. Solely for the purpose of showing line detections, we present in Fig.2 the on-source and of one of the two similar off-source spectra. These spec-

Table 1. Detected lines in IC1396N

λ_o (μm)	λ_v (μm)	Line id.	E_u (K)	IC1396N on	off
(1)	(2)	(3)	(4)	(5)	(6)
57.34	57.317	[NIII]	251	⋆	⋆
63.17	63.184	[OI]	228	⋆	⋆
69.04	69.072	H 12-11	1095	⋆	—
	69.074	CO 38-37	4080		
75.46	75.380	o-H_2O 3_{21}-2_{12}	304	⋆	—
84.53	84.411	CO 31-30	2736	⋆	—
	84.420	OH 7/2+-5/2- 4-3	290		
88.40	88.356	[OIII]	163	⋆	⋆
100.76	100.460	CO 26-25	1938	⋆	—
	100.913	o-H_2O 5_{14}-4_{23}	572		
104.65	104.445	CO 25-24	1794	⋆	—
108.45	108.073	o-H_2O 2_{21}-1_{10}	194	⋆	—
	108.763	CO 24-23	1657		
124.09	124.193	CO 21-20	1276	⋆	—
144.71	144.784	CO 18-17†	945	⋆	—
145.67	145.525	[OI]†	327	⋆	⋆
153.40	153.267	CO 17-16	846	⋆	—
157.74	157.741	[CII]	91	⋆	⋆
162.82	162.812	CO 16-15	752	⋆	—
173.64	173.631	CO 15-14†	664	⋆	—
174.63	174.626	o-H_2O 3_{03}-2_{12}†	197	⋆	—
179.69	179.526	o-H_2O 2_{12}-1_{01}	113	⋆	—
186.04	185.999	CO 14-13	581	⋆	—

Notes: Column (1) gives the observed wavelength; (2) the vacuum transition wavelength(s); (3) the line identification; (4) the energy of the upper level; (5 and 6) the detection on-source and in the two off-source positions.

Symbols: ⋆: detection; †: blended lines.

tra have been coadded, corrected for fringes with a preliminary procedure and their continua have been subtracted.

Table 1 lists the lines detected on-source and in the two off-source positions.

2.2. Millimeter and submillimeter observations

In March 1996, we observed the submillimeter continuum of IC1396N at the 15-m James Clerk Maxwell Telescope (JCMT), Mauna Kea, Hawaii, USA), using the UKT14 bolometer receiver (Duncan et al.1990). Calibration was referred to Uranus. Table 2 gives the effective wavelength of the observations,the corresponding beam FWHM and the observed flux densities and 1-σ errors (including absolute calibration uncertainties).

3. Discussion

3.1. The far infrared lines

From Table 1 and Fig.2 it can be seen that, while the molecular lines are detected only toward the IRAS source, the ionic lines are present at both the *on* and *off* source positions.

The ionic lines, with the exception of the [OI] lines, are uniformly bright at all positions, suggesting that they are emitted
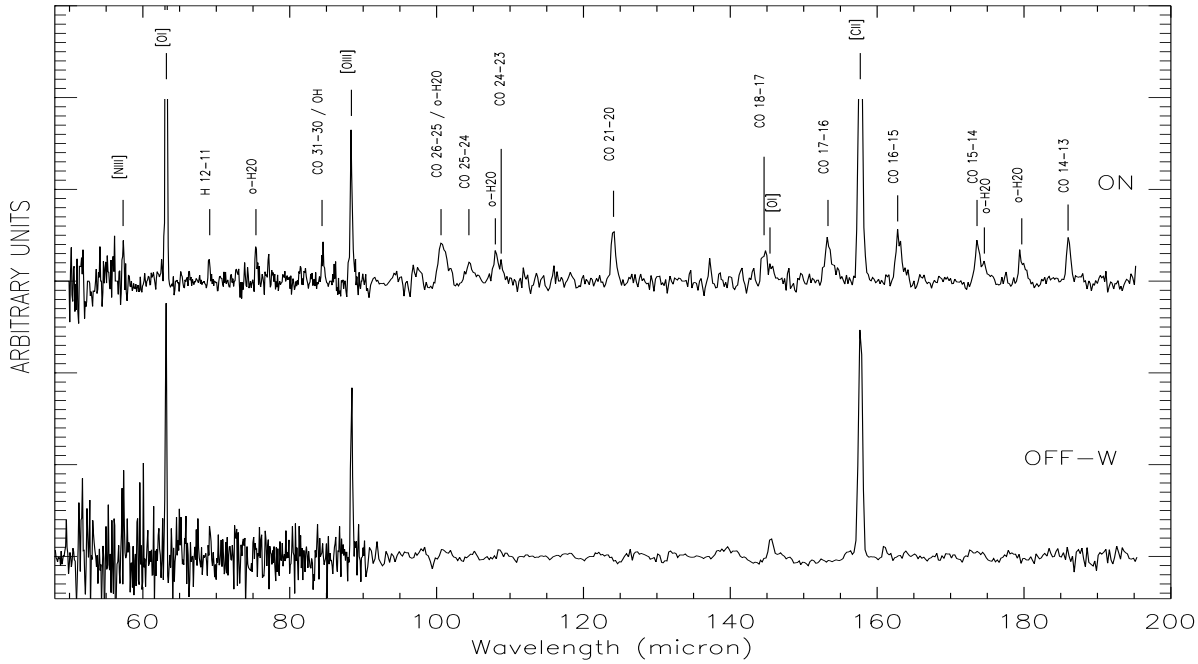
Fig. 2. The LWS spectra of IC1396N (upper) and its west *off*-source position (lower). The continuum emission has been subtracted. This figure is given only to show the line detection. Relative intensities among lines are not significant, because of the not yet reliable defringing procedure.

by the surrounding ISM and illuminated externally. The ubiquitous [CII] emission, seen in many sources (see e.g. Emery et al. 1996, Nisini et al. 1996) is also seen here, both on and off source. On the other hand, the intermediate ionization lines ([OIII] and [NIII]), require the presence of an ionizing source with a harder spectrum than that of IC1396N (L=235$L_\odot$, see next section). The obvious candidate is the O6 star HD 206267. The two [OI] lines are also seen in all the observed positions, but they peak on source. These lines may be excited by the same shocks that are suggested by the on-source detection of the molecular lines of CO, H_2O, and OH.

CO emission lines are clearly detected from transitions 14-13 through 25-24. The CO 26-25, 31-30 lines are blended with an H_2O and and OH line, respectively. The line at 69.1μm (at the same position of CO 38-37) is probably due mainly to the 12-11 hydrogen recombination line.

The high-J CO and H_2O emission imply relatively warm, dense gas associated with the IRAS source. Table 1 gives the excitation energies of the upper levels of the emitting transitions. The presence of water and OH lines indicates that these species are fairly abundant.

3.2. The continuum

The thermal emission spectrum of IC1396N is shown in Fig.3. The LWS spectrum has been derived by subtracting the average of the two off-source spectra from the on-source spectrum and scaling the resulting spectra for each detector to match overlapping data, leaving the SW3 flux fixed. This procedure produces

Table 2. (Sub)-millimeter Photometry of IC1396N

Wavelength (μm)	Beam ($arcsec$)	Flux (Jy)	Total Error (Jy)
350	19.0	73.8	8.7
450	17.5	39.2	4.3
800	16.0	5.17	0.36
1100	18.7	1.80	0.06
1300	19.1	1.38	0.10

good agreement with the 60 and 100μm IRAS fluxes and is consistent with the spectral shape observed with the JCMT.

The observed energy distribution (25-1300 μm) of IC1396N was fitted with a model consisting of a central heating source surrounded by a spherically symmetric dust envelope. This latter is modeled as a series of concentric shells in which density ρ and temperature T vary according to radial power laws, with exponents p and q, respectively. The boundary conditions on T and ρ are set at the outer envelope radius (T_{out}, ρ_{out}), which is assumed equal to 0.03 pc ($\sim$ 6000 AU), consistent with the CS J=5-4 map of Serabyn et al. (1993) and corresponding to roughly half of the JCMT beamsize. A dust mass opacity of 0.1 cm^2 g^{-1} at 250μm (Hildebrand 1983) is assumed, with the dependence on wavelength β as a free parameter.

The best fit to the data (Fig.3) gives the parameters: ρ_{out}=4.5 10^{-20} g cm^{-3}, T_{out}=23.5 K, q=0.36, p=0.5 and β=1.35 and a total gas+dust envelope mass (with a gas-to-dust ratio of 100) of 8.3M$_\odot$. Envelope radii larger than $\sim$ 0.03 pc would not be fit by any model, showing that the emitting region
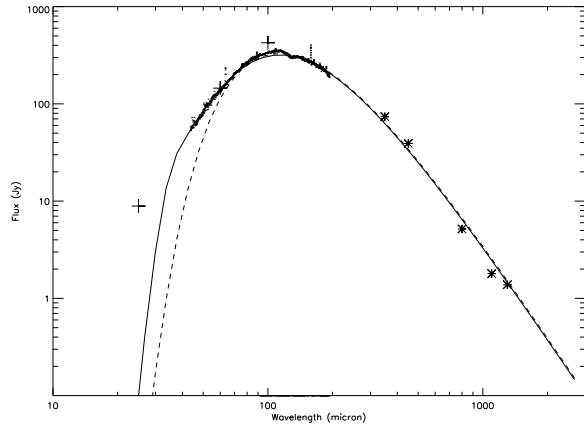
Fig. 3. Model fit to the continuum spectrum of IC1396N. Both the LWS and the JCMT data (stars) have been used for the fit. The 25, 60, and 100 μm IRAS fluxes are also given (crosses). The fits with density power law index $p=0.5$ (solid line), and $p=1.5$ (dashed line) are shown (see text).

is smaller than the JCMT beam, making, for this source, beam corrections unnecessary.

The obtained value of $p=0.5$ is lower than the one expected for a collapsing envelope ($p=1.5$). Similarly flat density profiles have been previously derived for YSOs (Barsony & Chandler 1993; André et al. 1993). The flat profile is constrained by the observed LWS spectrum shortward of 70μm, which requires relatively low optical depth (see in Fig.3 the fit with $p=1.5$). The temperature exponent, $q=0.36$, agrees with the values derived from radiative transfer calculations, ranging from $q=0.33$ (Butner et al. 1990) to $q \sim 0.5$ (Wolfire & Churchwell 1994).

The 25μm IRAS flux is not well fit by our model because we reach optically thick regimes for $\lambda \leq 40\mu$m. One possibility is that we overestimate the optical depth, using a single β value from the submillimeter to the mid-infrared. Besides, it may be that our model does not represent the real geometry of the source, because it does not consider a flattened structure.

We derive a bolometric luminosity of 235$L_\odot$, by integrating the observed spectrum from 12μm to 1.3mm, which well agrees with the value of Sugitani et al. (1989).

4. Conclusions

The main conclusions of this work are that:

- CO, OH and H_2O lines are detected toward the IRAS source associated with the bright rimmed globule IC1396N, revealing the presence of warm, dense material, probably excited by shocks;
- both *on-source* and *off-source* fine structure lines are present: the [OIII] and [NIII] lines are probably excited by the O6 star HD206267, while [OI] may be largely due to shock excited emission in the outflow;
- the continuum 25-1300 μm emission can be explained by the presence of an envelope of 8.3 $M_\odot$;

- a bolometric luminosity of 235 $L_\odot$ is derived from the continuum fit, in agreement with previous estimates.

References

André P., Ward-Thompson D., Barsony M. 1993, ApJ,406,122
Barsony M., Chandler C.J. 1993, ApJ,406, L71
Butner H.M. et al. 1990, ApJ,364,164
Clegg, P.E. et al. 1996, this volume
Dent W.R.F et al. 1989, MNRAS,238,1947
Duncan W.D. et al. 1990, MNRAS,243,126
Emery, R. et al. 1996, this volume
Hildebrand R.H. 1983, QJRAS 24,267
Kessler M. et al. 1996, this volume
Kun M., Balazs L.G., Toth I. 1987, ApSS,134,211
Matthews T.J. 1979, AA,75,345
Nisini B. et al. 1996, this volume
Patel N.A. et al. 1995,ApJ,447,721.
Osterbrock, D.E. 1957,ApJ,125,622
Serabyn E., Güsten R., Mundy L. 1993, ApJ,404,247
Simonson S.C. III 1968, ApJ,154,923
Sugitani K. et al. 1989, ApJ,342,47
Sugitani K., Fukui Y., Ogura K. 1991, ApJSS,77,59
Swinyard B. et al. 1996, this volume
Wolfire M.G., Churchwell E. 1994, ApJ,427,889